Magnetism of the tensile-strain-induced tetragonal state of $SrRuO_3$ films

A. Herklotz,[1,2] M. Kataja,[2] K. Nenkov,[2] M. D. Biegalski,[3] H.-M. Christen,[3] C. Deneke,[4] L. Schultz,[2] and K. Dörr[1]

[1]*Martin Luther University Halle-Wittenberg, Institute for Physics, Von-Danckelmann-Platz 3, 06120 Halle, Germany*

[2]*IFW Dresden, Institute for Metallic Materials, Helmholtzstraße 20, 01069 Dresden, Germany*

[3]*ORNL, Center for Nanophase Materials Sciences, Bethel Valley Road, Oak Ridge, Tennessee 37831-6496, USA*

[4]*Laboratorio Nacional de Nanotecnologia, Rua Giuseppe Maximo Scolfaro, 10000 Campinas, Sao Paulo 13083-100, Brazil*

(Received 28 March 2013; revised manuscript received 22 August 2013; published 14 October 2013)

$SrRuO_3$ films have been grown in the tetragonal, structurally single-domain state under 1% of biaxial tensile strain. The angular dependencies of the magnetization and the magnetoresistance reveal an upright orientation of the tetragonal unit cell and biaxial magnetic in-plane anisotropy with 110_t easy axes. Reversible biaxial strain from piezoelectric $Pb(Mg_{1/3}Nb_{2/3})_{0.72}Ti_{0.28}O_3$ (PMN-PT) substrates has been applied to probe the direct strain response of the magnetization and the electrical resistance. At 1% tensile strain, the Curie temperature (T_C) and the ordered magnetic moment (m_S) at low temperatures are found to substantially decrease with further growing tensile strain. This suggests a suppression of m_S resulting from distortions of the RuO_6 octahedra, in line with reported density-functional calculations. Reversible strain has also been applied to a film under weak tensile strain revealing the opposite response, i.e., an enhancement of T_C and m_S with tensile strain. Structural and magnetic properties of $SrRuO_3$ films in several static strain states (compressive, weak and strong tensile strain) are compared.

DOI: 10.1103/PhysRevB.88.144412 PACS number(s): 75.70.−i, 75.50.Bb, 75.47.Lx

I. INTRODUCTION

$SrRuO_3$ (SRO) has been used widely as electrode material in oxide heterostructures, mainly due to its excellent properties like good metallic conductivity and chemical stability. Apart from that it has also been the subject of extensive fundamental research in the recent years. In the following, three particularly interesting aspects are mentioned.

First, the degree of electron correlations and their impact on the physical properties has been long debated for SRO. For a 4*d* transition-metal oxide correlations are expected to be less pronounced than in the well-known 3*d* systems such as the manganites showing double-exchange ferromagnetism. Experimental results have suggested that electron-electron correlations play an important role as, for example, the observation of a metal-to-insulator transition in ultrathin films.[1] On the other hand, *ab inito* calculations reveal that SRO is a moderately correlated ferromagnet[2,3] and suggest that the experimental SRO thin-film properties may be induced by extrinsic factors.

Second, SRO is considered as a model system to study oxygen octahedral rotations in ABO_3 perovskites under strain and their effect on physical properties. This idea arose because bulk SRO has an ordered magnetic moment of about $1.6\mu_B$/f.u., which is close to the ideal value of $2\mu_B$ per Ru^{4+} ion, while $CaRuO_3$, having the same charge states but about twice as large octahedral rotations, has a vanishing ordered magnetic moment.[3,4] As strain is readily changing the bond angles between the octahedra, it is expected to have a strong impact on the thin-film magnetism. Vaillionis *et al.*[5] pointed out that SRO and $La_{0.66}Sr_{0.33}MnO_3$ (LSMO) thin films behave similarly under epitaxial strain and suggested that the observed lattice response to the epitaxial strain is of a general nature and can be applied to other perovskite-type materials. SRO has orthorhombic structure in bulk form, whereas LSMO is rhombohedral, yet in both cases a monoclinic structure is found under compressive strain and a tetragonal structure is obtained in tensile strained films.[6,7] However, the exact structure of the tetragonal phase in SRO remained under debate and a detailed characterization of the physical properties is lacking.

Third, SRO was shown to provide interesting phenomena at interfaces with manganites. A giant antiferromagnetic interlayer coupling with strong exchange bias[8,9] or enhanced magnetization[10] has been observed in superlattices comprised of $La_{0.7}Sr_{0.3}MnO_3$ and $SrRuO_3$. Antiferromagnetic coupling was also found in superlattices of $Pr_{0.7}Ca_{0.3}MnO_3$ and $SrRuO_3$.[11] Interestingly, SRO was shown to change its crystal symmetry from the bulklike orthorhombic structure to a tetragonal variant when the PCMO layer thickness was increased from 1.5 to 4 nm. At the same time the coupling strength was reduced.

All examples imply that a careful study of the interplay between the structural degrees of freedom and the magnetic properties of SRO is needed. In this work the effect of tensile strain on the structural, magnetic, and electric transport properties of single layers of SRO is investigated. Particular emphasis is placed on the characterization of tetragonal thin films. A combined approach of epitaxial misfit strain and piezoelectric substrate strain is used to carefully elucidate the effects of lattice distortions. The films are grown on (001) oriented substrates of $SrTiO_3$ (STO) and piezoelectric $Pb(Mg_{1/3}Nb_{2/3})_{0.72}Ti_{0.28}O_3$ (PMN-PT) covered with appropriate buffer layers in order to tune their as-grown strain state. Then, the strain of the films is reversibly and uniformly controlled by the inverse piezoelectric effect of the PMN-PT substrates.[12] In this way, the influence of biaxial strain on the magnetization and the resistance of prestrained $SrRuO_3$ films can be measured directly and quantitatively, independent of the effects of other parameters such as oxygen nonstoichiometry or microstructure.[13]

II. EXPERIMENT

SRO films have been grown on single-crystalline substrates of STO and PMN-PT with $Ba_xSr_{1-x}TiO_3$ buffer layers (BSTO)

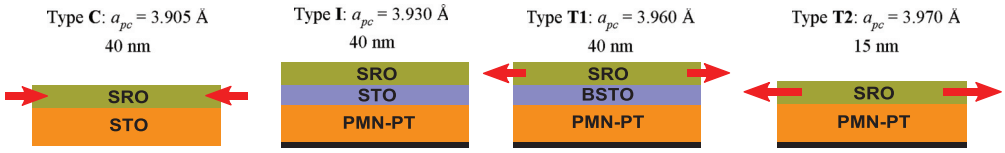

FIG. 1. (Color online) Schemes of the investigated samples with the $SrRuO_3$ film thickness and the pseudocubic in-plane lattice parameter noted. The different substrates [STO (**C**) and PMN-PT (**I, T1, T2**)] and buffer layers $Ba_xSr_{1-x}TiO_3$ with $x = 0$ for (**I**) and $x = 0.75$ for (**T1**) were used to control the strain state from compressed (**C**) to nearly relaxed (**I**) to tensile (**T**).

in order to achieve different strain states. The samples are represented in Fig. 1. The film growth was conducted by pulsed laser deposition (KrF 248 nm) from a stoichiometric target. The deposition temperature and the oxygen background pressure were 700 °C and 0.3 mbar, respectively. The films were annealed for 5 min and cooled down in 600 mbar of oxygen. Structural characterization and measurement of the film thickness have been carried out in a Philips X'Pert MRD diffractometer with Cu K_α radiation employing x-ray diffraction and reflectivity. The magnetization was measured in a superconducting quantum interference device (SQUID) magnetometer (Quantum Design). The Curie temperature was determined from temperature-dependent measurements of the remanent magnetization M by extrapolating the linear part of $M^2(T)$ to $M = 0$. For thin films this method systematically provides values that are reduced by a few K compared to measurements on bulk samples. Electrical transport measurements were performed using a standard four-terminal technique. During the reversible strain-dependent measurements an electrical field E_{piezo} is applied to the PMN-PT substrate between the conductive SRO film and a bottom electrode on the opposite (001) surface of the substrate in order to control the biaxial substrate strain.[14] In all cases measurements with positive and negative E_{piezo} were conducted and compared to each other to ensure that charge modulation is not an issue.

III. RESULTS AND DISCUSSION

A. Structural characterization

High resolution x-ray diffraction was employed to characterize the structure of the films. All films are grown epitaxially. The strain states of the films are determined by reciprocal space maps (RSMs) around the 103_s and 204_s substrate reflections. Cubic lattice indices are used for both substrates, STO and PMN-PT, and marked with the subscript "s." Even though poled PMN-PT is monoclinic, the deviations from a cubic lattice are small.[15] The pseudocubic lattice parameter of $SrRuO_3$ is 3.923 Å.[5] RSM around the $\{204\}_s$ lattice reflections of sample **C** demonstrate the coherent growth of the SRO film on the cubic STO substrate and reveal the previously reported orthorhombic symmetry.[6] Thus, the SRO film is under compressive in-plane strain. Table I summarizes its structural properties which agree with earlier work.[6,7] In previous studies it was pointed out that orthorhombic SRO films on STO substrates actually reveal a small monoclinic distortion as a result of the substrate constraint.[9,16]

The reciprocal space mapping on **T1** films reveal a noncoherent film growth of SRO on the BSTO buffer layer. However, a large tensile strain with an in-plane parameter of $a_{pc} = 3.96$ Å is maintained. In contrast to the case of the orthorhombic symmetry, the $\{h0l\}$ reflections appear at the same l position for a tetragonal structure with the c axis oriented along the surface normal. This feature is found in the tensile strained **T1** films as shown by the RSMs in Fig. 2. A tetragonal structure of SRO films grown on (110) oriented $DyScO_3$ and $GdScO_3$ substrates was evidenced earlier.[6,7] Here, a tetragonal structure is obtained for biaxially strained films grown on quasicubic (001) oriented PMN-PT substrates. The tetragonal c axis is found along the surface normal (as shown in more detail below). The lattice parameters are listed in Table I.

The **I** films with the intermediate strain state have been also investigated by reciprocal space mapping (data not shown). The $SrTiO_3$ buffer layer shows an enlarged in-plane lattice parameter ($a_{\text{STO}} = 3.93$ Å) compared to the bulk value as reported before.[17] The SRO layer grows coherently onto the buffer with $a_{pc} = 3.93$ Å. This lattice parameter agrees with that of a film studied by Terai *et al.*[18] Hence, the **I** state films show a weak tensile strain. They are likely to exhibit tetragonal symmetry as the **T1** state films as will be concluded from angular-dependent magnetization and anisotropic magnetoresistance measurements below. Due to an overlap of the SRO and STO lattice reflections it is hard to rule out the existence of some orthorhombic domains or a small orthorhombic distortion.

Two different orientations of the orthorhombic (monoclinic) or tetragonal unit cells have to be distinguished because of their strong impact on magnetism: (I) the in-plane

TABLE I. List of structural and magnetic properties as function of strain state. For sake of comparison the lattice parameters are given in unit-cell dimensions analogous to the bulk structure of SRO.

Sample	**C**	**I**	**T1 (T2)**
a_{pc} (Å)	3.905	3.93	3.96 (3.97)
Biaxial strain	Compressive	Weak tensile	Tensile
(%)	−0.46	0.19	0.94 (1.20)
Symmetry	Orthorhombic	Tetragonal	Tetragonal
Epitaxial orientation	$[110]_o//[001]_s$ $[001]_o//[100]_s$	$[001]_t//[001]_s$ $[100]_t//[011]_s$	$[001]_t//[001]_s$ $[100]_t//[011]_s$
a (Å)	5.549	5.565	5.590 (5.605)
b (Å)	5.569	5.565	5.590 (5.605)
c (Å)	7.81	7.838	7.82 (7.81)
$V \sim a \cdot b \cdot c$ (Å^3)	241.35	242.74	244.36 (245.36)
T_C	149.1	150.0	153.5
$dT_C/d\epsilon$		1.9	−6.2
Easy axes	Tilted out-of-plane	$[110]_t$, $[1\underline{1}0]_t$	$[110]_t$, $[1\underline{1}0]_t$
$\Delta M_S/M_S$ ($\Delta\epsilon = 1\%$)		6%	−9%

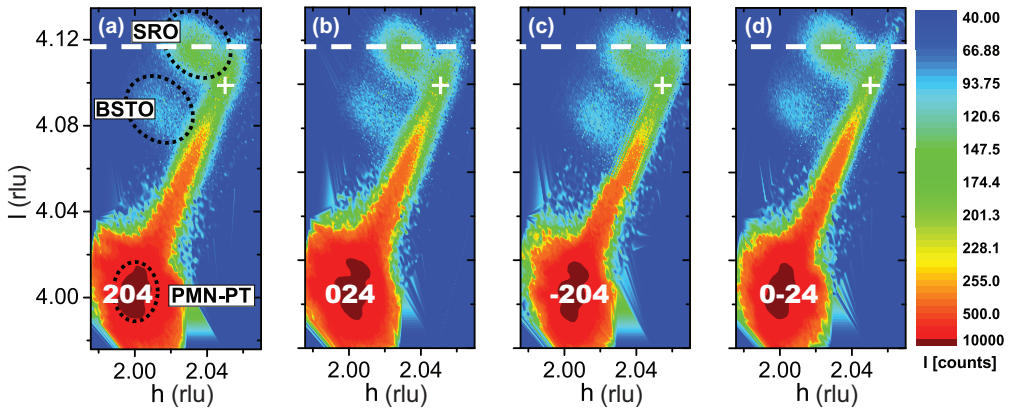

FIG. 2. (Color online) Reciprocal space maps around the $\{204\}_s$ lattice reflections of a sample of type **T1**. The reciprocal-lattice units are in terms of the PMN-PT pseudocubic bulk lattice parameter. The white crosses mark the position of a virtual cubic film with the pseudocubic lattice parameter of bulk SRO, $a = 3.923$ Å.

orientation with the c axis $[001]_{o/t}$ lying in the film plane along a $[100]_s$ axis and the diagonal $[110]_{o/t}$ lying approximately along the film normal and (II) an out-of-plane oriented c axis with the a and b axis in the film plane. The epitaxial relationship (I) was previously found in the orthorhombic SRO films on STO.[9] Due to the pseudocubic nature of SRO the two possible tetragonal orientations are nearly degenerate and hard to distinguish by laboratory-scale x-ray diffraction.[19] Here, we analyze the angular dependence of the anisotropic magnetoresistance (AMR) in order to clarify the structure and epitaxial relationship for films under compressive and tensile strains.

Magnetotransport measurements were performed by rotating the samples around the 100_s and 010_s in-plane axes of the substrates in a magnetic field of $\mu_0 H = 7$ T both at 10 and 130 K. The current $\boldsymbol{I}$ has been parallel to the axis of rotation and perpendicular to the magnetic field always. The magnetoresistance is defined as $MR = [\rho(7T) - \rho(0)]/\rho(0)$. The monoclinic, orthorhombic, or tetragonal symmetry of the films determines the angular dependence of the magnetoresistance as pointed out in Ref. 20. To be more specific, the magnetoresistance $\Delta\rho/\rho$ can be expressed in terms of a series of sine and cosine functions,

$$\Delta\rho/\rho(\theta) = c_0 + \sum_{n=1}^{\infty} s_{4n-2}\sin[(4n-2)\theta] + \sum_{n=1}^{\infty} c_{4n}\cos(4n\theta), \quad (1)$$

$$\Delta\rho/\rho(\theta) = c_0 + \sum_{n=1}^{\infty} c_{2n}\cos(2n\theta), \quad (2)$$

$$\Delta\rho/\rho(\theta) = c_0 + \sum_{n=1}^{\infty} s_{2n}\sin(2n\theta) + \sum_{n=1}^{\infty} c_{2n}\cos(2n\theta), \quad (3)$$

where θ is the angle between the direction of the magnetic field and the film normal. If a monoclinic C_{2h} symmetry with the epitaxial relationship (I) is considered, the magnetoresistance for $\boldsymbol{I}//[1\bar{1}0]_m$ and $\boldsymbol{I}//[001]_m$ can be expressed by Eqs. (2) and (3), respectively. In the case of an orthorhombic symmetry the magnetoresistance for $[\boldsymbol{I}//1\bar{1}0]_o$ is expressed by Eq. (2) and the magnetoresistance for $\boldsymbol{I}//[001]_o$ is expressed by Eq. (1). For a tetragonal film with out-of-plane oriented c axis, both the magnetoresistance with $\boldsymbol{I}//[110]_t$ and $[\boldsymbol{I}//1\bar{1}0]_t$ are described by Eq. (2). Therefore, by measuring the magnetoresistance for rotations of the magnetic field about both pseudocubic in-plane axes, conclusions on the structural symmetry of the films can be made.

Figures 3(a) and 3(b) shows the measured AMR for a **C** film at 130 K with rotations around 100_s and 010_s, respectively. The data in Fig. 3(a) are representative for an orthorhombic or monoclinic structure, i.e., the data can be fitted by Eq. (2). However, the data for the rotation along the other principal axis is approximated by (1), but can only be fitted adequately when Eq. (3) is used. It is therefore evident that our films grown on STO substrates adopt an orthorhombic structure with a small monoclinic distortion as reported earlier. We also want to note that the positions of the maxima in Fig. 3(b) at about 50° and 230° are related to the specific easy axis orientation in compressed SRO films. The magnetic anisotropy will be discussed later.

In our measurements for the **T** state we observe an equal angular dependence for the two in-plane rotational axes [Figs. 3(c) and 3(d)], hinting strongly to a fourfold in-plane symmetry and an upright tetragonal cell as described by Eq. (2). Fit curves are included in Figs. 3(c) and 3(d) and work well. It has to be noted that a mixed state with an equal amount of tetragonal domains oriented in both in-plane directions could result in the same AMR pattern. Nevertheless, we find this scenario rather unlikely, since one domain orientation is usually favored over the other, e.g., due to the presence of large miscut (∼3°) as found in our PMN-PT substrates.

In addition to these structural studies XRD measurements using synchrotron light have been conducted on a strongly tensile strained **T2** film in order to examine the structural response of the film under variable piezoelectric substrate strain. In this approach out-of-plane diffraction around $(00l)$ and grazing incidence in-plane diffraction around $(k00)$ reflections are used to track changes of the lattice parameters of both the PMN-PT substrate and the film. A voltage supplied to the piezoelectric substrate was used to control the substrate's biaxial strain. From the changes of a and c the Poisson's ratio of the film has been

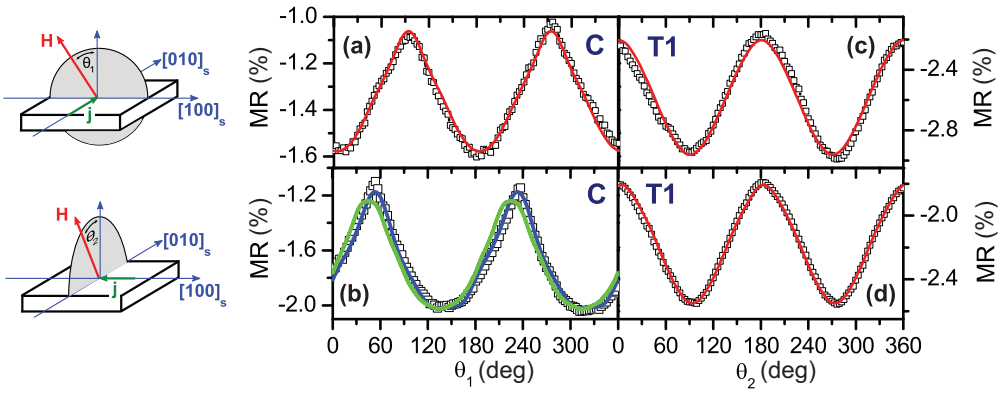

FIG. 3. (Color online) Angular dependent magnetoresistance of a **C** film (left side) and a **T1** film (right side) at 130 K in a field of 7 T. In (a) and (c), the magnetic field was rotated within the $(010)_s$ plane and in (b) and (d) the field was rotated within the $(100)_s$ plane. The current was always perpendicular to the magnetic field. The solid red lines are fits of the expression in Eq. (2). The good agreement with the data for both current directions is a fingerprint of tetragonal symmetry in **T** films. The solid green and blue lines are fits to the expressions in (1) and (3), respectively, and are used to identify orthorhombic and monoclinic symmetry in **C** films, as explained in the text.

determined.[15] The measurements on the initial state of the SRO film are in line with a tetragonal unit cell as found for the **T1** films, with pseudocubic lattice parameters of $a = 3.963$ Å and $c = 3.905$ Å. Upon application of an electric field the piezoelectric substrate is contracting in plane, consequently leading to a relief of tensile strain of the SRO film by the same amount and an expansion of the lattice along the film normal. From the variation of the in-plane and out-of-plane lattice parameters δa and δc we have calculated the Poisson's ratio of SRO to be $\nu = \frac{\delta_c}{\delta_c - 2\delta_a} = 0.28 \pm 0.02$. This value is in the typical range found for many nonferroelectric perovskites. This agrees with density functional calculations of the strain-dependent lattice parameter by Zayak *et al.*,[16] from which a Poisson's ratio of $\nu = 0.32$ can be estimated.

B. Magnetism

In this section we focus on the magnetism of the tensile-strain SRO films, since the compressed state on STO has been analyzed before.[9,21,22] We find T_C values of 153.5 K for the **T1**-type samples, a value which is slightly smaller than the SRO bulk value of about 160 K.[23] The **C**-type and **I**-type samples have a T_C of 149.1 and 150.0 K, respectively. We note that the conducted measurements of T_C in remanence provides lower values than in-field measurements. For the magnetic moment per formula unit (m_S) measured at 4.5 T we find different values depending on whether the magnetic field is perpendicular or parallel to the film plane. This observation has been reported many times before and is attributed to the fact that SRO can hardly be saturated due to the strong magnetocrystalline anisotropy.[9] Moreover, paramagnetic contributions of SRO in high magnetic fields have been discussed.[24] In thin films, it is difficult to separate the substrate contribution (which is commonly assumed to be diamagnetic, possibly giving rise to another error) to the measured magnetic moment for the case of a nonsaturated film magnetization. Our measured values lie in the range published in literature before, which is rather wide. Therefore, we abstain from reporting values for the saturated magnetic moment of our SRO films.

The strain dependence of both T_C and the magnetic moment have been probed in reversible-strain runs for the **T1**- and **I**-state films on piezoelectric substrates. In order to measure the strain dependence of the magnetic moment per formula unit, measurements must be performed in a geometry that does not result in magnetization rotation. Since rotation may happen for all noneasy directions because of the large magnetocrystalline anisotropy of SRO, the measurements must be conducted along an easy axis. Therefore, rotational SQUID magnetometry was employed prior to the reversible strain measurements in order to identify the orientation of the magnetic easy axes in the tetragonal lattice.

Figure 4 shows the angular dependence of the magnetization of a **T1** film in a field of $\mu_0 H = 1.5$ T at 10 K both during rotation about an in-plane 100_s axis [Fig. 4(a)] and the 001_s substrate normal [Fig. 4(b)]. In Fig. 4(a), maxima of the magnetization are observed when the field is applied in the film plane, i.e., along 010_s. A similar curve has been obtained for the rotation about the other in-plane axis, 010_s. For the in-plane rotation of the field [Fig. 4(b)], four rather equal maxima appear for the field along the 100_s directions. These angular dependencies show that the 110_t and $1\text{-}10_t$ directions of the tetragonal unit cell coincide with the easy axes of the film. We note that the same orientation of the easy axis has been determined from measurements on the **I** films, indicating the same tetragonal structure and orientation as found for the **T** films.

For reversible strain measurements, a magnetic field of 0.1 T has been applied during cooling along an in-plane 100_s direction of the substrate in order to induce a remanent magnetization. At stepwise increasing temperatures the substrate was biaxially compressed by applying a substrate electric field of 10 kV/cm. The resulting relative change of the remanent magnetization, $\Delta M/M$, is shown in Fig. 5. We find that the magnetoelastic response is composed of two components for both cases of measured film types, the **T1** films and the **I** films. One contribution shows a peak behavior close to the Curie temperature and is vanishing at low temperatures (light red and blue area), whereas the other part is present at low temperatures and considered to be constant in the whole temperature range (dark red and blue).

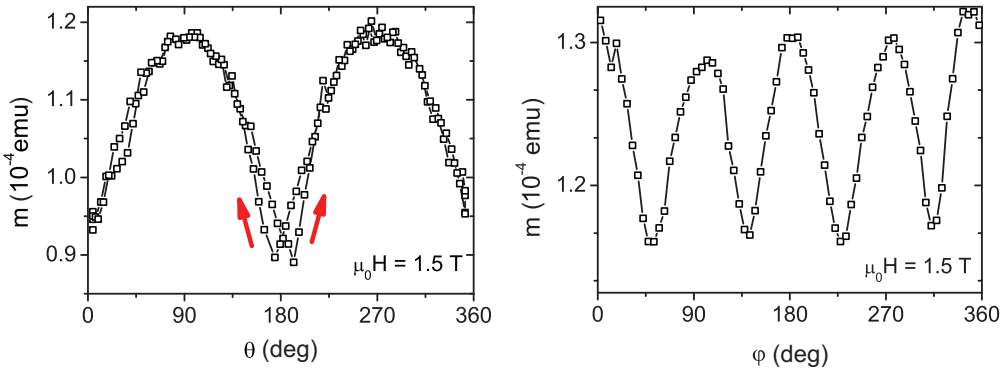

FIG. 4. (Color online) Angular dependencies of magnetization in a **T1** film with the field rotating about the 100_s axis (left) and in the film plane about the 001_s axis (right). θ and φ are the angles between the magnetic field and the 001_s and 100_s axis, respectively. The measurements were done at 10 K in a magnetic field of $\mu_0 H = 1.5$ T. In the first measurement the data were recorded rotating back and forth to check for magnetic hysteresis as highlighted by the red arrows.

The first effect has been found in ferromagnetic manganites and cobaltites before,[12,25] and has been attributed to the strain-induced change of the Curie temperature. It has been shown that the strain-induced shift of the Curie temperature can be estimated fairly well based on the temperature-dependent $M(T)$ curve and the measured $\Delta M/M$ data as described in Ref. 13. For the **T**-state film, the magnetoelastic response $\Delta M/M$ is positive near T_C and corresponds to a strain-induced shift of the Curie temperature of $dT_C/d\epsilon \sim -6.2$ K/%. The **I**-state film, on the other hand, exhibits a negative magnetoelastic response near T_C and the strain effect on T_C is estimated to be $dT_C/d\epsilon \sim +1.9$ K/% (Table I). Here, a piezoelectric strain of $\epsilon = -0.08\%$ was assumed for the applied electric field of 10 kV/cm at about 140 K. The magnitude of the piezoelectric strain obtained for the constant electric field is somewhat temperature dependent as reported in Ref. 14. At 300 K, $\epsilon = -0.11 \pm 0.01\%$ has been determined by x-ray diffraction with

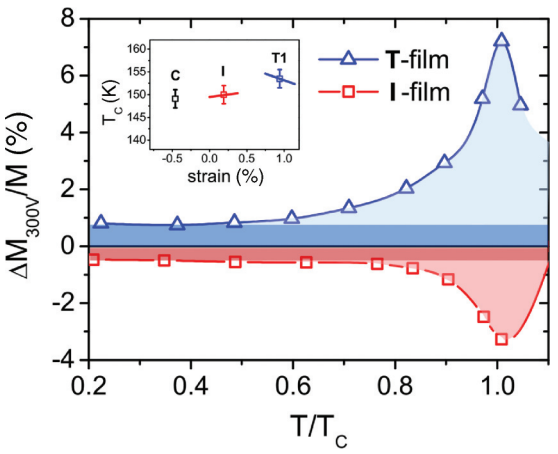

FIG. 5. (Color online) Temperature dependence of the strain-induced M change for the strain states with substrate fields of $E_{\text{piezo}} = 0$ and 10 kV/cm, recorded for an **I** film (red) and for a **T1** film (blue). The measurements were conducted in remanence after field cooling in $\mu_0 H = 0.1$ T, in-plane along a direction 100_s. The dashed lines indicate the Curie temperatures of the films. The meaning of the colored areas are explained in the text. The inset illustrates the dependence of T_C on the biaxial strain.

in situ applied electric field of 10 kV/cm for a typical PMN-PT substrate,[15] and the strain decreases slightly between 300 K and about 60 K, followed by a more pronounced decrease towards the lowest temperature of 30 K applied in this work.

As a consequence of the contrasting behavior of the strain effect on T_C it can be concluded that the ferromagnetic ordering temperature possesses a maximum between the two strain states of the **I** and the **T1** film, i.e., at a pseudocubic in-plane parameter of about 3.94–3.95 Å. Our results are in agreement with earlier work[18,26] in that a growing T_C was found for a (small) tensile strain as present in the **I** films.

The second contribution (dark colored areas) in $\Delta M/M$ which is assumed to be independent of temperature is attributed to the influence of the strain on the ordered magnetic moment. We note that the introduction of the two contributions is motivated by the temperature dependence of the spontaneous magnetization, $M_S(T,\epsilon) = M_S(T=0,\epsilon) \times f[T/T_C(\epsilon)]$, with a shape function f assumed to be constant under the small applied piezoelectric strain.[27] In the $T1$ state, the magnetization grows at all temperatures upon partial release of the tensile strain, whereas it is decreasing at all temperatures for the I-type film. The changes derived from the temperature-independent component (dark shaded areas in Fig. 5) are $\Delta M/M$ −9% and +6% per percent of strain for the **T1**-type and the **I**-type film, respectively, and are attributed to changes of m_S (which is proportional to the spontaneous magnetization M_S). A rotation of the local magnetization orientation or a shift of a domain wall caused by the biaxial in-plane compression is excluded by having measured in remanence along one of the four symmetric in-plane easy axes for both types of films. Thus, the strain-induced change of m_S can be ascribed to two possible physical origins: (i) an influence on the spin orientation and degree of spin order or (ii) a variation of the magnetic moments themselves. (We note that this is an appropriate view for localized magnetic moments. The alternatives are not clearly distinguishable in a band model and would not need consideration.)

For case (i), collinear magnetic order in the SRO ground state is commonly assumed, but we could not find a confirmation by direct evidence such as a neutron-diffraction study. A noncollinear order might change under the applied strain. Nonideal magnetic order could also result from an imperfect

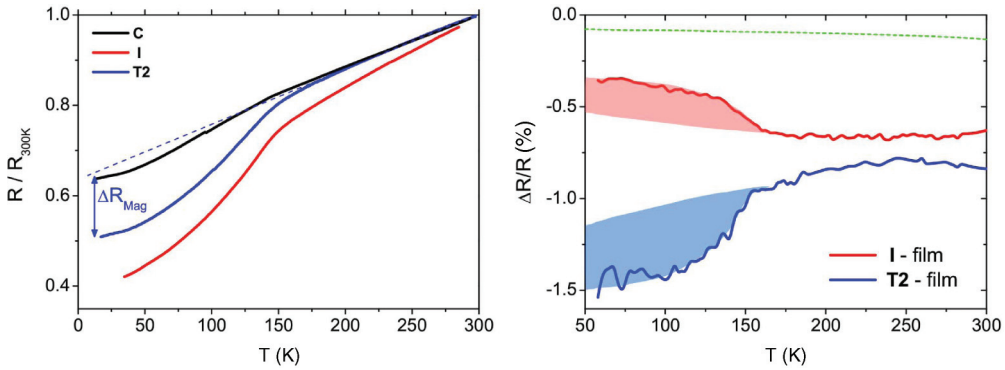

FIG. 6. (Color online) (a) Temperature dependence of the electric resistance normalized to the room-temperature value for films in the **C**, **I**, and **T2** states with the current direction along the 100_s axis. (b) Strain-induced change of the resistance between $E_{\text{piezo}} = 0$ and 10 kV/cm for an **I** and a **T2** film. The colored area indicates the contribution that is related to the ferromagnetic alignment as explained in the text. The dashed green line indicates the resistance change from the bare change of the geometry (length and cross section).

film microstructure/defects, but the observed effect in $\Delta M/M$ seems too substantial for this being the major origin. Hence, case (i) is less likely even though it is not strictly ruled out.

For the more likely case (ii), i.e., a strain-induced variation of the magnetic moment, we tried to compare our data to published calculations of the magnetic moment vs strain. Zayak *et al.*[16] calculated the strain dependence of the magnetic moment for (001) oriented SRO with orthorhombic *Pbnm* and tetragonal *P4/mmm* symmetry. Our data for the **T** state agrees qualitatively and even quite well quantitatively with the tetragonal *P4/mmm* case. On the other hand our result for the **I** state clearly disagrees with the calculations for this symmetry. Note that in the tetragonal structure with *P4/mmm* symmetry rotations and tilts of the oxygen octahedra are absent. According to Choi *et al.*[7] this structure is found in tensile strained SRO films grown on (110) oriented $DyScO_3$ substrates. However, the situation might be different for (001) oriented substrates. The tetragonal symmetry in a film does not rule out the presence of rotations or tilts. Vailionis *et al.*[5] pointed out that tetragonal films under tensile strain show no rotations of the octahedra around the $[001]_t$ direction, but tilts around both in-plane axes are present. This structure was favored, since it preserves the in-plane octahedral rotation pattern of the orthorhombic structure during the transition to the tetragonal state. To the best of our knowledge there is no calculation of the magnetic moment published for a tetragonal structure including this octahedral tilt system. The octahedral rotations around the $[110]_t$ and $[1\underline{1}0]_s$ directions depend on the magnitude of the mismatch and are expected to decrease with increasing tensile strain until they are greatly diminished when the substrate's in-plane lattice constant exceeds the doubled Ru-O bond length of the film.[5] Then, the structure is close to the simple tetragonal *P4/mmm* perovskite structure, which might explain the good agreement of our data from the heavily strained **T1** film with the calculations by Zayak *et al.*[16] for the tetragonal *P4/mmm* structure devoid of rotations or tilts of the oxygen octahedra.

C. Electric transport

The electric transport properties of $SrRuO_3$ films have been shown to be affected by epitaxial strain, as for example revealed by Gan[28] *et al.* or Vaillionis.[6] However, the exact influence remained somewhat uncertain. In the latter case, films have been deposited in different strain states onto several different substrates and may have a different defect structure affecting the resistance. In the former case, the removal of the film from the substrate in order to get a strain-free $SrRuO_3$ layer may have introduced microcracks causing the rather large change of resistance. Figure 6(a) shows temperature-dependent resistance measurements normalized to the room temperature value for our SRO films. The typical "bad metal" behavior, i.e., a linear decrease, is found for lowering the temperature from room temperature towards T_C. During cooling through T_C all resistance curves exhibit a drop, which is most pronounced for the **I**-state film and least pronounced for the compressively grown **C** film. This change of the resistance, here denoted as ΔR_{Mag} [marked in Fig. 6(a)], is clearly related to the onset of the ferromagnetic order and was attributed to the reduction of spin-dependent scattering.[29] As mentioned earlier, SRO shows a quite pronounced angular dependent magnetoresistance with a minimum of the resistance in a parallel magnetic field configuration. Bearing in mind that in zero field the magnetization is not in the film plane for the **C**-type film, but somewhat tilted to the film normal, while for the other strain states it is, it can be expected to see the smallest ΔR_{Mag} for the **C** film.

The direct strain response of the resistance was measured for **I** and **T2** films. Figure 6(b) shows the relative change of the resistivity upon a release by tensile strain of about 0.1%. The strain effect is negative over the entire examined temperature range for both film types. This finding is in agreement with the previous studies by Gan[28] and Vaillionis.[6] A decrease of the resistivity of up to 7.5% per 0.1% in-plane strain was found comparing a SRO film deposited on $DyScO_3$ to a film deposited on $SrTiO_3$. Here, where the strain is applied reversibly after film growth, rather than induced by growth onto different substrates, the magnitude of the strain effect is considerably smaller. We determine a reduction of less than 1.5% per 0.1% in-plane strain. The strain effect on the resistivity originates from two different contributions. The first one is related to the change of the magnetization and is therefore only apparent below the Curie temperature [see blue and red areas in Fig. 6(b)]. For the **I** film spin-dependent

scattering is enhanced when the magnetization is reduced along the in-plane easy axis [Fig. 5(a)] with the induced compressive strain. In contrast, the resistivity is reduced for the **T** film due to the reversed effect of strain on the magnetization. The second contribution is negative, present also well above the ferromagnetic ordering temperature and of the same order of magnitude for both films. A reduction of the resistivity above T_C due to compressive strain was also found by Vailionis *et al.*[6] and attributed to the reduction of electron correlations or the increase of the one-electron bandwidth as a consequence of changed Ru-O-Ru bond angles.

IV. SUMMARY AND CONCLUSION

The structural, magnetic, and electric transport properties of $SrRuO_3$ films in substrate-induced biaxial strain states, with particular emphasis on strong tensile strain were studied. It was shown that small biaxial strain (in the **I**-state films) introduces a tetragonal structure which is present up to 1% tensile strain. The c axis of the tetragonal unit cell is oriented out of plane and, therefore, these films are structurally single domain with $\langle 110\rangle_t \parallel \langle 100\rangle_s$. The magnetic easy axes are in plane along the $\langle 110\rangle_t$ directions. Direct measurements of the strain-dependent magnetization along an easy axis, achieved by applying reversible strain from a piezoelectric PMN-PT substrate, reveal that both the Curie temperature and the ordered magnetic moment decrease (grow) with increasing tensile strain for the case of strong (weak) tensile strain. It is concluded that T_C exhibits a maximum in the tetragonal phase for a pseudocubic in-plane lattice parameter of 3.94–3.95 Å. The strain-induced decrease of the magnetization at low temperatures under strong tensile strain suggests a suppression of the ordered Ru magnetic moment resulting from distortions of the RuO_6 octahedra, in line with earlier reported density-functional calculations. Reversible strain measurements of the electric resistance show a smaller impact of strain than reported previously, of the order of 10% resistance change per 1% of strain. This is consistent with the weaker electron correlations in $SrRuO_3$ if compared, e.g., to the lanthanum manganites which show much stronger response of electrical transport to strain.[30] Our results provide a basis for a better understanding of oxide heterostructures containing SRO layers under tensile strain. However, for completing the fundamental issue of the strain response of $SrRuO_3$, the exact pattern of the octahedral rotations in dependence on strain has yet to be clarified.

ACKNOWLEDGMENTS

The authors would like to acknowledge the support of DFG FOR520 and the Scientific User Facilities Division, Office of Basic Energy Sciences, US DOE. We thank A. Malachias for assistance at the Brazilian National Synchrotron Light Laboratory–LNLS.

[1] D. Toyota, I. Ohkubo, H. Kumigashira, M. Oshima, T. Ohnishi, M. Lippmaa, M. Takizawa, A. Fujimori, K. Ono, M. Kawasaki *et al.*, Appl. Phys. Lett. **87**, 162508 (2005).

[2] J. M. Rondinelli, N. M. Caffrey, S. Sanvito, and N. A. Spaldin, Phys. Rev. B **78**, 155107 (2008).

[3] I. I. Mazin and D. J. Singh, Phys. Rev. B **56**, 2556 (1997).

[4] A. T. Zayak, X. Huang, J. B. Neaton, and K. M. Rabe, Phys. Rev. B **77**, 214410 (2008).

[5] A. Vailionis, H. Boschker, W. Siemons, E. P. Houwman, D. H. A. Blank, G. Rijnders, and G. Koster, Phys. Rev. B **83**, 064101 (2011).

[6] A. Vailionis, W. Siemons, and G. Koster, Appl. Phys. Lett. **93**, 051909 (2008).

[7] K. J. Choi, S. H. Baek, H. W. Jang, L. J. Belenky, M. Lyubchenko, and C.-B. Eom, Adv. Mater. **22**, 759 (2010).

[8] X. Ke, M. S. Rzchowski, L. J. Belenky, and C. B. Eom, Appl. Phys. Lett. **84**, 5458 (2004).

[9] M. Ziese, I. Vrejoiu, E. Pippel, P. Esquinazi, D. Hesse, C. Etz, J. Henk, A. Ernst, I. V. Maznichenko, W. Hergert *et al.*, Phys. Rev. Lett. **104**, 167203 (2010).

[10] P. Padhan, W. Prellier, and R. C. Budhani, Appl. Phys. Lett. **88**, 192509 (2006).

[11] M. Ziese, I. Vrejoiu, E. Pippel, A. Hahnel, E. Nikulina, and D. Hesse, J. Phys. D: Appl. Phys. **44**, 345001 (2011).

[12] K. Dörr, O. Bilani-Zeneli, A. Herklotz, A. D. Rata, K. Boldyreva, J. W. Kim, M. C. Dekker, K. Nenkov, L. Schultz, and M. Reibold, Eur. Phys. J. B **71**, 361 (2009).

[13] A. Herklotz, A. D. Rata, L. Schultz, and K. Dörr, Phys. Rev. B **79**, 092409 (2009).

[14] A. Herklotz, J. D. Plumhof, A. Rastelli, O. G. Schmidt, L. Schultz, and K. Dorr, J. Appl. Phys. **108**, 094101 (2010).

[15] M. D. Biegalski, K. Dörr, D. H. Kim, and H. M. Christen, Appl. Phys. Lett. **96**, 151905 (2010).

[16] A. T. Zayak, X. Huang, J. B. Neaton, and K. M. Rabe, Phys. Rev. B **74**, 094104 (2006).

[17] O. Bilani-Zeneli, A. D. Rata, A. Herklotz, O. Mieth, L. M. Eng, L. Schultz, M. D. Biegalski, H. M. Christen, and K. Dörr, J. Appl. Phys. **104**, 054108 (2008).

[18] K. Terai, T. Ohnishi, M. Lippmaa, H. Koinuma, and M. Kawasaki, Jpn. J. Appl. Phys. **43**, L227 (2004).

[19] R. J. Kennedy, R. Madden, and P. A. Stampe, J. Phys. D **34**, 1853 (2001).

[20] M. Ziese, I. Vrejoiu, and D. Hesse, Phys. Rev. B **81**, 184418 (2010).

[21] A. Grutter, F. Wong, E. Arenholz, M. Liberati, A. Vailionis, and Y. Suzuki, Appl. Phys. Lett. **96**, 082509 (2010).

[22] X. W. Wang, X. Wang, Y. Q. Zhang, Y. L. Zhu, Z. J. Wang, and Z. D. Zhang, J. Appl. Phys. **107**, 113925 (2010).

[23] J. Neumeier, A. Cornelius, and J. Schilling, Physica B **198**, 324 (1994).

[24] S. Kolesnik, Y. Z. Yoo, O. Chmaissem, B. Dabrowski, T. Maxwell, C. W. Kimball, and A. P. Genis, J. Appl. Phys. **99**, 08F501 (2006).

[25] A. D. Rata, A. Herklotz, K. Nenkov, L. Schultz, and K. Dorr, Phys. Rev. Lett. **100**, 076401 (2008).

[26]M. Wissinger, D. Fuchs, L. Dieterle, H. Leiste, R. Schneider, D. Gerthsen, and H. V. Löhneysen, Phys. Rev. B **83**, 144430 (2011).

[27]C. Thiele, K. Dörr, O. Bilani, J. Rödel, and L. Schultz, Phys. Rev. B **75**, 054408 (2007).

[28]Q. Gan, R. A. Rao, and C. B. Eom, Appl. Phys. Lett. **70**, 1962 (1997).

[29]L. Klein, J. S. Dodge, C. H. Ahn, J. W. Reiner, L. Mieville, T. H. Geballe, M. R. Beasley, and A. Kapitulnik, J. Phys.: Condens. Matter **8**, 10111 (1996).

[30]M. C. Dekker, A. Herklotz, L. Schultz, M. Reibold, K. Vogel, M. D. Biegalski, H. M. Christen, and K. Dörr, Phys. Rev. B **84**, 054463 (2011).